Efficient numerical simulation of ac conduction in heterogeneous materials at low temperatures

Muhammad Sahimi,[1] Maryam Naderian,[2] and Fatemeh Ebrahimi[1,3]
[1]*Department of Chemical Engineering, University of Southern California, Los Angeles, California 90089-1211, USA*
[2]*Institute for Advanced Studies in Basic Sciences, Gava Zang, Zanjan 45195-159, Iran*
[3]*Department of Physics, Faculty of Sciences, University of Birjand, Birjand 97178-51367, Iran*
(Received 1 November 2004; published 30 March 2005)

The problem of computing the effective frequency-dependent conductivity of heterogeneous materials at low temperatures is studied. In this problem the activation energies and, therefore, the local conductivities (or the transition rates in a master equation formulation) are broadly distributed, varying over many orders of magnitude. Such broad variations make the computations with large lattices that represent the materials very difficult. We use an efficient method, based on computing the wavelet scale and detail coefficients of the local conductivities, in order to compute the effective ac conductivity of such materials. The method identifies the high-conductance paths in a large lattice and reduces it to one that requires far less computation. Using the method, we compute the effective ac conductivity of a two-dimensional lattice in which the activation energies are distributed according to a probability distribution function (PDF). Five distinct PDFs are used, and the effective ac conductivity is computed over many orders of magnitude variations in the frequency. Depending on the size of the initial system, the speedup in the computations for two-dimensional systems varies anywhere from a factor of 35–40 to over 200.

DOI: 10.1103/PhysRevB.71.094208 PACS number(s): 66.30.Dn, 66.30.Hs, 72.20.−i

I. INTRODUCTION

Transport processes in heterogeneous materials constitute an important set of phenomena that are relevant to a wide variety of problems in natural and industrial processes. Examples include flow in porous media, conduction and hopping transport in, and mechanical properties of, heterogeneous solid materials,[1] and many more. In particular, predicting the frequency-dependent effective conductivity of electronically or ionically conducting heterogeneous materials has been a problem of great interest for several decades.[2,4] Measurements of the ac conductivity of such disordered solids as amorphous semiconductors, polymers, and ionically conductive glasses indicate a number of common characteristics:[2] For frequencies larger than a characteristic frequency ω_m, the effective conductivity $\sigma_e(\omega)$ becomes strongly frequency dependent and follows a power law

$$\sigma_e(\omega) \sim \omega^x, \tag{1}$$

where the exponent x is a decreasing function of the temperature with $0.6 \leqslant x \leqslant 1.0$.[2,4] The characteristic frequency ω_m is proportional to the dc conductivity, $\omega_m \propto \sigma_e(0)$, a relation known as the Barton-Nakajima-Namikawa law.[5,6] Moreover, examining the vast amount of experimental data for the ac conductivity of a wide variety of disordered materials indicates that most of the data follow a universal representation[7,8] given by

$$\hat{\sigma} = \frac{\sigma_e(\omega)}{\sigma_e(0)} = F\left[\epsilon_0 \Delta\epsilon \frac{\omega}{\sigma_e(0)}\right]. \tag{2}$$

Here, ϵ_0 is the vacuum permeativity, $F(x)$ is a universal function, and $\Delta\epsilon = \epsilon(0) - \epsilon_\infty$, with $\epsilon(0)$ and ϵ_∞ being, respectively, the zero-frequency and bound-charge dielectric constants of the materials.

In order to explain the experimental data, several models of ac conduction have been developed in the past. The most thoroughly studied model is perhaps the hopping model[2–4] which describes jumps of charge carriers in a stochastic medium, typically represented by a lattice. The model is described by the following master equation for the probability $P_i(t)$ of finding a charge carrier at site i:

$$\frac{\partial P_i(t)}{\partial t} = \sum_{\{j\}} [W_{ij} P_j(t) - W_{ji} P_i(t)], \tag{3}$$

where W_{ij} is the transition rate, i.e., the probability of making a jump from site i to site j, and $\{j\}$ denotes the set of all the sites to which a jump occurs. To take into account the effect of a material's disorder, it is usually assumed that the transition rates are exponential functions of an activation energy and/or a tunneling distance, and that they are nonzero only for nearest-neighbor jumps. Hopping models, described by Eq. (3), are complex. Except for one-dimensional (1D) materials, no exact solution of Eq. (3) is known. Thus, to estimate the effective ac conductivity several approximations have been developed. An early and relatively simple one was the continuous-time random walk model of Scher and Lax,[9] which is similar to a mean-field Hartree-type approximation.[10,11] A widely used approach is the effective-medium approximation[10,12,13] and the related methods.[14] Although such approximations provide a qualitative picture of many properties of the ac conductivity, they are not very accurate for obtaining precise estimates of $\sigma_e(\omega)$.

We also point out that although hopping models have been used for describing ac conduction in disordered solids, the physics behind such models and that of the macroscopic continuum-type models are quite different.[2–4] However, subject to certain assumptions, the formal mathematical formu-

lations of the hopping models and the macroscopic approaches are rather similar (see also below).

Numerical simulation of ac conduction in heterogeneous materials is a difficult problem. The difficulty is twofold. (1) Hopping models usually assume noninteracting charge carriers, as they ignore the self-exclusion effect that allows at most one charge carrier per site of the lattice, as well as the Coulomb interactions between the carriers. When such effects are explicity accounted for, the resulting model becomes very complex.[15] (2) The exponential dependence of the transition rates on the activation energy and/or a tunneling distance implies that they are very broadly distributed, often over many orders of magnitude variations. Under these conditions, computer simulation of ac conduction is difficult, particularly in 3D for which there is still a lack of precise numerical results obtained with large systems.[2] Although Dyre[16] carried out numerical simulation of ac conduction in both 2D and 3D in which the effect of the Coulombic interaction was taken into account, her simulations were restricted to relatively small systems. The transfer-matrix method has also been used[17] for computing the ac conductivity. However, the system studied was restricted to one near the percolation threshold in which the local conductivities were either zero or 1.

In this paper, we use a highly efficient method for numerical simulation of ac conduction in heterogeneous materials. The method is ideally suited for the cases in which the transition rates are distributed over many orders of magnitude, and can be used with very large lattices in both 2D and 3D. The method is based on two key facts. (1) In a heterogeneous material in which the local conductivities are distributed over many orders of magnitude, only a small subset of the material contributes significantly to its overall effective conductivity. (2) If portions of the material are characterized by low local conductivities, there is no need to represent them in the model by a detailed lattice structure; instead, one can coarsen such zones of the system. The method used in this paper takes advantage of these two facts. We show that, starting with a large lattice for which a very large number of equations must be solved in order to determine the electrostatic potential distribution and estimate its effective ac conductivity, we can systematically reduce the system to one for which only a relatively small number of equations should be solved, hence drastically reducing the computation time.

The plan of this paper is as follows. In the next section we formulate the problem that we wish to solve in this paper. Section III describes the method that we propose for solving the governing equations, while the results are presented and discussed in Sec. IV.

II. THE MODEL

In this section we set up the governing equations for ac conduction in a heterogeneous material with spatially varying (frequency-independent) conductivities,[18] following Dyre.[16] We assume that the material has free charge carriers characterized by a local conductivity $g(\mathbf{r})$, as well as bound charges described by a fixed dielectric constant $\epsilon_\infty = \epsilon_e(\omega \to \infty)$. The basic constitutive equations are given by

$$\mathbf{D}(\mathbf{r},t) = -\epsilon_\infty \nabla V(\mathbf{r},t), \tag{4}$$

$$\mathbf{J}(\mathbf{r},t) = -g(\mathbf{r}) \nabla V(\mathbf{r},t). \tag{5}$$

Here, $\mathbf{D}$ and $\mathbf{J}$ are, respectively, the displacement and free-charge-carrier current flux, and V is the electrostatic potential. If $\rho(\mathbf{r},t)$ is the density of the free charge carriers, we must have (Gauss's law),

$$\nabla \cdot \mathbf{D}(\mathbf{r},t) = \rho(\mathbf{r},t), \tag{6}$$

which, together with the continuity equation

$$\frac{\partial \rho(\mathbf{r},t)}{\partial t} + \nabla \cdot \mathbf{J}(\mathbf{r},t) = 0, \tag{7}$$

yields the governing equation for the electrostatic potential $V(\mathbf{r},t)$,

$$\nabla \cdot \left[\epsilon_\infty \frac{\partial}{\partial t} \nabla V(\mathbf{r},t) + g(\mathbf{r}) \nabla V(\mathbf{r},t) \right] = 0. \tag{8}$$

Note that using Gauss's law implies that Coulombic interactions are (implicitly) taken into account. In a periodically varying potential field, all the quantities are written as functions of $\mathbf{r}$ times $\exp(i\omega t)$. Thus, Eq. (8) becomes

$$\nabla \cdot \{[s + g(\mathbf{r})] \nabla V(\mathbf{r},s)\} = 0, \tag{9}$$

where $s = i\omega\epsilon_\infty$. If we now use a standard finite-difference approximation to discretize Eq. (9), we obtain a d-dimensional simple-cubic lattice in which each bond consists of a resistor and a capacitor in parallel. A bond's admittance is $y(\mathbf{r}) = \alpha[s + g(\mathbf{r})] = \alpha[i\omega\epsilon_\infty + g(\mathbf{r})]$, where α is a constant. It is not difficult to show that $\alpha = \ell^{d-2}$, where ℓ is the lattice constant. If the local conductivity $g(\mathbf{r})$ varies continuously, then the above discretization is exact when the lattice constant $\ell \to 0$.

We assume that the local conductivity $g(\mathbf{r})$ is thermally activated, and that its spatial variation is due to the activation energy E varying in space, so that

$$g(\mathbf{r}) = g_0 \exp[-\beta E(\mathbf{r})], \tag{10}$$

where $\beta = (k_B T)^{-1}$, with k_B and T being the Boltzmann constant and the temperature. The activation energy $E(\mathbf{r})$ changes spatially because the local structure of the solid material varies. In many cases one expects $E(\mathbf{r})$ to vary little. However, our focus in this paper is the low-temperature limit where $g(\mathbf{r})$ varies over orders of magnitude. In addition, the local activation energies are typically not random, but correlated with a correlation length ξ_E. However, we set the lattice constant $\ell = \xi_E$ and ignore all the correlations beyond the lattice constant ℓ. In this way, the local conductivities $g(\mathbf{r})$ become uncorrelated. This assumption can, of course, be relaxed, if need be. If two opposing faces of the lattice are identified with two electrodes and short circuited, and if a potential drop ΔV is imposed between the two electrodes, the resulting current is $I(s) = Y_e(s)\Delta V$, where $Y_e(s)$ is the effective admittance of the lattice. The effective conductivity $\sigma_e(s)$ is then given by

$$\sigma_e(s) = L^{2-d} Y_e(s) - s, \tag{11}$$

where L is the length of the system.

III. NUMERICAL SIMULATION

Consider, first, the problem of ac conduction in a continuous system. We define the wavelet transformation (WT) of the admittance $y(\mathbf{r})$ by

$$D(a,\mathbf{b}) = \int_{-\infty}^{\infty} y(\mathbf{r}) \psi_{ab}(\mathbf{r}) d\mathbf{r}. \tag{12}$$

Here, $\psi_{ab}(\mathbf{r}) = \psi[(\mathbf{r}-\mathbf{b})/a]/\sqrt{a}$, with $a>0$ being a rescaling parameter and $\mathbf{b}$ representing translation of the wavelet. The function $\psi(\mathbf{r})$ is called the *mother wavlet*. Equation (12) indicates that, by using a WT transformation of $y(\mathbf{r})$, utilizing a shifted and rescaled wavelet, one can analyze its distribution at increasingly coarser ($a>1$) or finer ($a<1$) length scales. This implies that, given an appropriate scheme, one can compress information on the spatial distribution of $y(\mathbf{r})$ at any length scale of interest since, as is well known, the WT of $y(\mathbf{r})$ contains information on the *difference* between two approximations of the same admittance function in two successive (one finer and one coarser) length scales. On the other hand, the most accurate estimate of the average of $y(\mathbf{r})$ at a *fixed* scale is obtained by using the *wavelet scaling function* $\phi(\mathbf{r})$, which is orthogonal to $\psi(\mathbf{r})$. Then, the wavelet approximate or scale coefficients of $y(\mathbf{r})$ are defined by

$$S(a,\mathbf{b}) = \int_{-\infty}^{\infty} \phi_{ab}(\mathbf{r}) y(\mathbf{r}) d\mathbf{r}, \tag{13}$$

where the definition of $\phi_{ab}(\mathbf{r})$ is similar to that of $\psi_{ab}(\mathbf{r})$. $\psi_{ab}(\mathbf{r})$ and $\phi_{ab}(\mathbf{r})$ are related, so that specifying one yields the other.[19]

In this paper we represent a disordered material by an $M \times M$ square lattice in which the conductivities $g(\mathbf{r})$, and thus the admittances $y(\mathbf{r})$, are distributed randomly [by distributing the activation energies $E(\mathbf{r})$]. Hence, we must use a discrete WT (DWT) [so that the parameters a and $\mathbf{b}$ of the wavelet $\psi_{ab}(\mathbf{r})$ take on discrete values]. We number the bonds and represent them by their centers which, hereafter, are referred to as the "nodes." Alternatively, we may view the system as a lattice of square blocks, each of which is characterized by an admittance $y(\mathbf{r})$. Then, if $\mathbf{r}=(k_1,k_2)$ represents the node of bond number n, associated with the DWT at $\mathbf{r}$ are four wavelet coefficients, three of which are given by

$$D_j^{(\ell)}(k_1,k_2,n) = \int_{\Omega} y(\mathbf{r},n) \psi_{j,k_1,k_2}^{(\ell)}(\mathbf{r}) d\mathbf{r}, \tag{14}$$

with $\ell=1$, 2, and 3 measuring the contrasts between $y(\mathbf{r})$ in the coarser scale [the one in which the length of a bond of admittance $y(\mathbf{r})$ is twice larger than the initial lattice that we start with] and those of its neighbors in the previous finer scale in the x, y, and diagonal directions, respectively. Here, j (the analog of the parameter a in the continuous WT) is the level of compression, such that the large lattice that models the system is represented by $j=1$, and Ω is the domain of the problem. The fourth wavelet coefficient is defined by

$$S_j(k_1,k_2,n) = \int_{\Omega} y(\mathbf{r},n) \phi_{j,k_1,k_2}(\mathbf{r}) d\mathbf{r}. \tag{15}$$

To carry out the numerical simulations, we proceed as follows. Since at a fixed frequency the imaginary part of the complex admittance $y(\mathbf{r}) = \alpha[i\omega\epsilon_\infty + g(\mathbf{r})]$ is constant, it is more convenient to work directly with the conductivities $g(\mathbf{r})$. Therefore, we first compute the scale and detail coefficients of the conductivities, and normalize them by their corresponding maximum values in the lattice. Two thresholds $0<t_s<1$ and $0<t_d<1$ are then defined for the wavelet scale and detail coefficients. The (normalized) scale coefficient $S_j(k_1,k_2,n)$ of each bond, represented by a node at $\mathbf{r}=(k_1,k_2)$, is then examined. If $S_j(k_1,k_2,n)>t_s$ (implying that the conductivity, and therefore the admittance, at $\mathbf{r}$ is large), we examine the scale coefficient of the next bond in the list. If, however, $S_j(k_1,k_2,n)<t_s$, we examine the (normalized) wavelet detail coefficients associated with that bond, and set to zero those for which $D_j^{(\ell)}(k_1,k_2,n)<t_d$. Physically, $D_j^{(\ell)}(k_1,k_2,n)=0$ means that the neighbor of the bond centered at (k_1,k_2) and corresponding to the direction (ℓ), which is just one bond (or one diagonal) away from the one centered at (k_1,k_2), is combined with its neighbor (see below). This procedure then eliminates many nodes (bonds) and combines them with their neighbors, the number of which depends on the broadness of the spatial distribution of $g(\mathbf{r})$. If the statistical distribution of $g(\mathbf{r})$ is broad, the compressed parts of the system are scattered throughout the lattice. The newly compressed lattice represents the system at the level $j=2$, and is referred to as the *current* lattice.

The current lattice is again compressed by applying the DWT to its scale coefficients and calculating a new set of four wavelet coefficients for each of its nodes. The new detail coefficients are again set to zero if they are smaller than t_d, and the corresponding nodes in the current (level $j=2$) lattice are combined with their neighbors. This process is repeated again until no significant number of the nodes are eliminated. The resulting lattice represents the system at the compression level $j=3$. Typically, the lattice at the compression level $j=4$ or 5 can no longer be effectively compressed, hence yielding very efficiently the final reduced lattice for fixed t_s and t_d. The numerical values of the thresholds are fixed by the desired precision of the results and, hence, the amount of computation time that we can afford. Note that the final compressed lattice is usually a mixture of larger and smaller square blocks, since some parts of the lattice for which $D_j^{(\ell)}<t_d$ join up and form larger square blocks. One must carefully treat those regions of the lattice in which the smaller and larger square blocks are neighbors, so as to avoid generating unphysical features, such as disconnected smaller and larger blocks (or nodes) that in reality are connected, since a bond or node is not physically eliminated (that is, its admittance is not set to zero); rather, it is simply combined with its neighbors.

Each time the current lattice is compressed, one must assign new effective admittances to the bonds (or the corre-

sponding nodes) of the newly compressed system. This can be done by reconstructing the distribution of the bonds' conductivities or admittances in the reduced lattice, i.e., by computing the *inverse* DWT of the conductivity or admittance distribution *after* the reduction and assigning the local admittances based on the reconstructed distribution. A simpler method, which is what we used in this paper, is based on the law of electrical circuits. In effect, each time a node in each direction is removed, one must compute the equivalent admittance of four nodes representing a simple four-block (or four-node) configuration, with each of the blocks having their own admittances, which are then replaced, after compression, by an equivalent admittance.

IV. RESULTS AND DISCUSSION

We have carried out computer simulations using 1024×1024 lattices. In all the cases, we have solved the problem using both the original 1024×1024 lattices, as well as those obtained by applying the DWT which reduces drastically the number of equations to be solved (see below). A comparison between the two sets of results provides an indication for the accuracy of the method. To solve the governing equations for the electrostatic potentials $V(\mathbf{r},s)$ throughout the lattice [the discretized version of Eq. (9)], we used the biconjugate-gradient method. All the results presented below represent averages over ten different realizations of the lattices, representing, to our knowledge, the largest 2D systems and the most extensive simulations for estimating the ac conductivity of 2D disordered materials. The most extensive simulations were carried out for the results presented below which were obtained at temperature $\beta=(k_BT)^{-1}=60$, using the thresholds $t_d=t_s=0.7$, and many orders of magnitude variations in the frequency, although less extensive simulations were also carried out at a few other low temperatures and using $t_d=0.5$ and $t_s=0.9$. The qualitative features of the results in all the cases were the same as those presented below. Following Dyre,[16] five distinct probability distribution functions (PDFs) $P(E)$ of the activation energies E were utilized, which are as follows.

(1) *Asymmetric Gaussian* distribution,

$$P(E) = \sqrt{\frac{2}{\pi}}\exp\left(-\frac{1}{2}E^2\right), \quad 0 < E < \infty; \tag{16}$$

(2) *Cauchy* distribution,

$$P(E) = \frac{2}{\pi}\frac{1}{1+E^2}, \quad 0 < E < \infty; \tag{17}$$

(3) *exponential* distribution,

$$P(E) = \exp(-E), \quad 0 < E < \infty; \tag{18}$$

(4) *power-law* distribution,

$$P(E) = 3(1+E)^{-4}, \quad 0 < E < \infty; \tag{19}$$

(5) *uniform* distribution,

$$P(E) = 1, \quad 0 < E < 1. \tag{20}$$

These PDFs result, in all the cases, in conductivities that are distributed over at least 5–6 orders of magnitude variations. Note that since the conductivities $g(\mathbf{r})$ are distributed at random, the percolation threshold of the system is $p_c=1/2$. Therefore, the critical energy E_c at which a sample-spanning cluster of the conducting bonds is formed is given by $1/2=\int_{-\infty}^{E_c}P(E)dE$, which results in[16] $E_c=0.674$, 1, 0.693, 0.26, and 0.50 for the distributions (16)–(20), respectively.

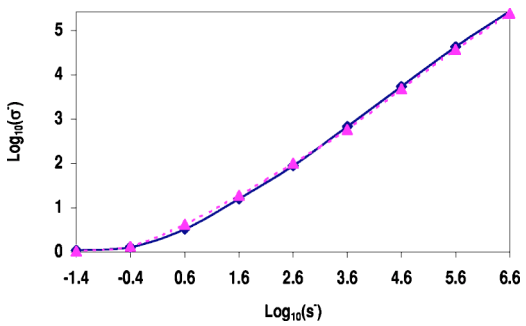

FIG. 1. Comparison of the (dimensionless) effective conductivity $\hat{\sigma}$, computed using the initial 1024×1024 lattice (diamonds, connected by the continuous curve), with that obtained with the rescaled lattice (triangles, connected by the dashed curve). The PDF of the activation energies is asymmetric Gaussian.

Figure 1 compares the frequency-dependent conductivity $\hat{\sigma}=\sigma_e(s)/\sigma_e(0)$, computed using the 1024×1024 lattice, with those calculated based on the reduced lattices, using the asymmetric Gaussian distribution of the activation energies. The quantity $s=i\omega$ has been made dimensionless through, $\hat{s}=[\beta/d\sigma_e(0)]s$. In this figure and those discussed below the continuous and dashed curves represent, respectively, guide to the eyes for the numerical results (represented by the symbols) obtained with the 1024×1024 and the reduced lattices. As can be seen, over eight orders of magnitude variations in the frequency, there is very little difference between the two sets of results. Figure 2 presents the same, but obtained with the Cauchy distribution of the activation energies. Once again, the agreement between the two sets of results is excellent. This case is particularly important, as the Cauchy distribution has a divergent variance and, therefore, is difficult to use in the numerical simulations.

The results obtained with the exponential, power-law, and uniform distributions of the activation energies are presented, respectively, in Figs. 3–5. The largest difference between the two sets of results is for the power-law distribution, and is no more than 1–3 %. The agreement between the two sets of

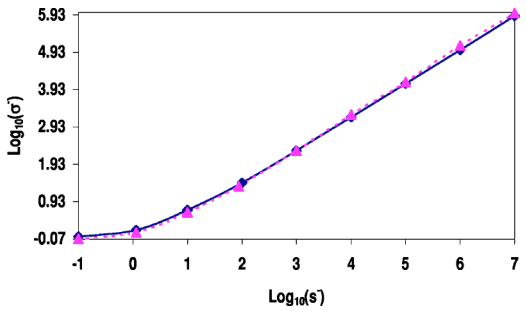

FIG. 2. Same as in Fig. 1, but for the Cauchy distribution of the activation energies.

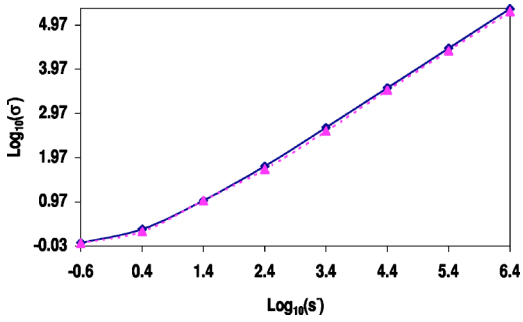

FIG. 3. Same as in Fig. 1, but for the exponential distribution of the activation energies.

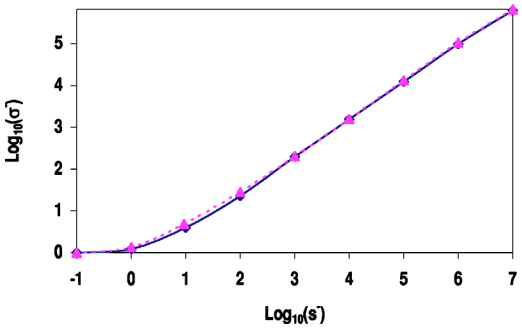

FIG. 5. Same as in Fig. 1, but for the uniform distribution of the activation energies.

results in all the cases demonstrates the accuracy of the method. Moreover, as the results indicate, the method's accuracy is independent of the range of the frequency and the PDF of the activation energies.

In Fig. 6 we rescale all the results of Figs. 1–5 according to Eq. (2), where $\hat{\omega}=[\epsilon_0\Delta\epsilon/\sigma_e(0)]\omega$. All the results have collapsed onto an essentially single curve which, over a broad range of $\hat{\omega}$, appears to be a straight line, hence supporting Eq. (1). Figure 6 provides further strong support for the universality of ac conductivity of a broad class of heterogeneous materials.[2,4,7,8]

How efficient is the method that we have used in this paper? Computing the wavelet transformation of the conductivity $g(\mathbf{r})$ is done highly efficiently, and represents only about 1% of the total computation time. Hence, the greatest savings are obtained through compressing and rescaling the lattice and, therefore, by reducing the number of equations that one must solve in order to determine the potential distribution in the lattice. In Fig. 7 we present the frequency dependence of the quantity N_c/N, where N_c is the number of equations that we solved in the reduced lattice, while $N=1\,046\,528$ is the number of equations that were solved to determine the electrostatic potential distribution in the initial 1024×1024 lattice. It is seen that, over a very broad range of the frequencies and for the five distinct PDFs of the activation energies, the ratio N_c/N is at most about 0.029. That is, instead of solving over a million equations for each frequency, one solves *at most* about 30 000 equations, if the thresholds $t_d=t_s=0.7$ are used, a factor of 35 reduction in the number of the equations to be solved and, hence, a computational speedup by at least the same factor. Using $t_d=t_s=0.9$ reduces the number of equations to be solved to only about 5 000, with the accuracy of the results being comparable with what is shown in Figs. 1–5. This would represent a factor of about 200 in savings in the computation time. In fact, the larger is the initial lattice model, the larger will be the computational speedup.

Our preliminary simulations in 3D indicate that even larger savings in the computation time than those reported here for 2D systems can be obtained. This is particularly important, as there is currently a lack of precise numerical results for the effective ac conductivity of 3D systems, obtained using large lattices.[2]

At this point, two important aspects of the method that we use in this paper are worth discussing.

(1) In a previous paper,[20] we suggested a method for efficient simulation of transport in heterogeneous media based on grid coarsening, which also used a WT. However, in that method only the wavelet detail coefficients were computed for grid compression, as the method was intended for disordered media in which there is long-range correlation between the local transport properties. Due to the correlation, clusters of large or small conductivities are formed, as a result of which compressing the lattice based only on the wavelet detail coefficients sufficed, since the wavelet detail coefficients

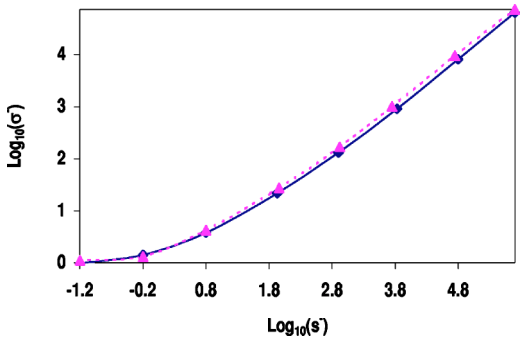

FIG. 4. Same as in Fig. 1, but for the power-law distribution of the activation energies.

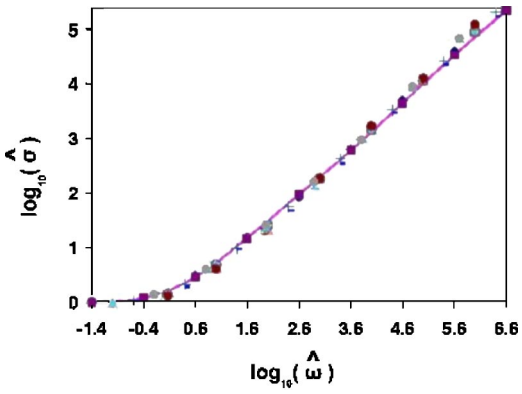

FIG. 6. Rescaled conductivities of Figs. 1–5 versus rescaled frequencies. Symbols represent the results for asymmetric Gaussian (diamonds and squares), Cauchy (open and filled circles), exponential (+ and black −), power-law (gray − and circles), and uniform (triangles and ×) PDFs, where the symbols in parentheses represent, respectively, the results for the initial and rescaled lattices.

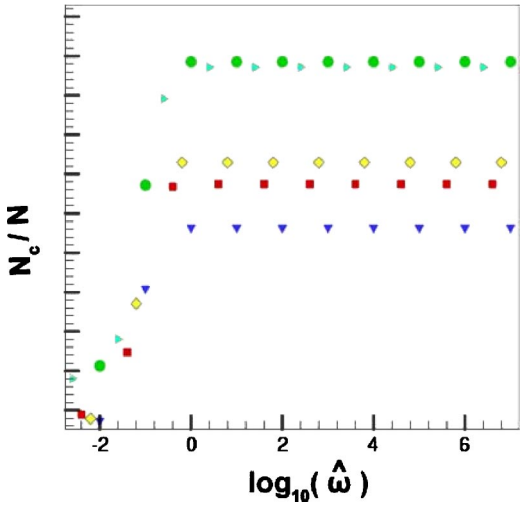

FIG. 7. Dependence of N_c/N on the rescaled frequency, where N_c and N are, respectively, the number of equations solved with the compressed and initial lattices. Symbols are the same as in Fig. 6.

characterize the *contrast* between different clusters or zones of the system in two consecutive scales, which for correlated media is the most important property. However, when we applied the method proposed in Ref. 20 to the present problem, it yielded poor results, since the bond conductivities in the problem studied in this paper are distributed randomly (without any correlation). The reason is that in the present problem not only are the contrasts between the conductivities important, but so also are the *magnitudes* of the local $g(\mathbf{r})$ or $y(\mathbf{r})$, which necessitate computing the wavelet scale coefficients that characterize the average magnitude of g or y at a *fixed scale*.

(2) The lattice compression that the WT carries out, which generates a grid with fewer but larger blocks, is reminiscent of the rescaling of the lattice models of critical and percolation phenomena by the position-space renormalization group (PSRG) methods.[21] In fact, we believe that the method that we describe in this paper can be thought of as a type of *inhomogeneous* PSRG method in that the blocks of the initial lattice are rescaled as in a PSRG method, but by different rescaling factors that the method chooses "intelligently" based on the wavelet scale and detail coefficients. Therefore, it should be interesting to make a qualitative comparison between the present method and the PSRG techniques. For 2D systems, the PSRG methods provide accurate estimates of the effective conductivity of materials with percolation disorder.[22] However, they are not easy to extend to frequency-dependent properties, or to media in which the local conductivities are distributed according to a broad PDF. On the other hand, as demonstrated in the present paper, the WT-based method provides accurate estimates of $\sigma_e(\omega)$ at any frequency and for any PDF of the local conductivities or admittances. At the same time, the PSRG methods are not very accurate for 3D media, unless they are combined with Monte Carlo simulations, whereas the WT-based method is as accurate and efficient in 3D as it is in 2D systems.

The WT-based method offers another important advantage over all of the previous methods in that it provides a way of generating grids of unequal block sizes for simulation of transport processes in any complex systems, so long as a property of the system varies spatially. For example, one can use the WT-based method for simulation of turbulent transport and photochemical reactions in the atmosphere over a vast area[23] (of the order of several thousands of square kilometers) and involving tens of reactants, or for simulation of multiphase flows in field-scale porous media,[24] and obtain numerical results with accuracies that are comparable with those obtained with massively parallel computational strategies.

ACKNOWLEDGMENTS

The authors are grateful to many colleagues, and in particular Ramin Golestanian, Amir Heidarinasab, M. R. H. Khajehpour, and Ehsan Nedaaee Oskoee, for very useful discussions and help in the computations.

[1] S. Torquato, *Random Heterogeneous Materials* (Springer, New York, 2002).
[2] J. C. Dyre and T. B. Schrøder, Rev. Mod. Phys. **72**, 873 (2000); C. Léon, A. Rivera, A. Várez, J. Sanz, J. Santamaria, and K. L. Ngai, Phys. Rev. Lett. **86**, 1279 (2001).
[3] H. Böttger and V. V. Bryskin, *Hopping Conduction in Solids* (Akademie-Verlag, Berlin, 1985).
[4] M. Sahimi, *Heterogeneous Materials* (Springer, New York, 2003), Vol. 1, Chap. 6.
[5] J. L. Barton, Verres Réfract. **20**, 328 (1966); T. Nakajima, in *1971 Annual Report, Conference on Electric Insulation and Dielectric Phenomena* (National Academy of Sciences, Washington, D.C., 1972), p. 168; H. Namikawa, J. Non-Cryst. Solids **18**, 173 (1975).
[6] J. C. Dyre, J. Non-Cryst. Solids **88**, 271 (1986).
[7] D. L. Sidebottom, Phys. Rev. Lett. **82**, 3653 (1999).
[8] T. B. Schrøder and J. C. Dyre, Phys. Rev. Lett. **84**, 310 (2000).
[9] H. Scher and M. Lax, Phys. Rev. B **7**, 4491 (1973); **7**, 4502 (1973).
[10] T. Odagaki and M. Lax, Phys. Rev. B **24**, 5284 (1981).
[11] J. C. Dyre, J. Non-Cryst. Solids **135**, 219 (1991).
[12] V. V. Bryskin, Fiz. Tverd. Tela (Leningrad) **22**, 2441 (1980) [Sov. Phys. Solid State **22**, 1421 (1980)]; I. Webman, Phys. Rev. Lett. **47**, 1496 (1981); S. Summerfield, Solid State Commun. **39**, 401 (1981).
[13] M. Sahimi, B. D. Hughes, L. E. Scriven, and H. T. Davis, J. Chem. Phys. **78**, 6849 (1983); B. D. Hughes, M. Sahimi, L. E. Scriven, and H. T. Davis, Int. J. Eng. Sci. **22**, 1083 (1984); M. Sahimi, J. Phys. C **19**, 1311 (1986).
[14] B. Movaghar and W. Schirmacher, J. Phys. C **14**, 859 (1981); S. Summerfield and P. N. Butcher, *ibid.* **15**, 7003 (1982).
[15] P. Maass, J. Petersen, A. Bunde, W. Dieterich, and H. E. Roman,

Phys. Rev. Lett. **66**, 52 (1991).
[16] J. C. Dyre, Phys. Rev. B **47**, 9128 (1993); **48**, 12 511 (1993); **49**, 11 709 (1994).
[17] J. M. Laugier, J. P. Clerc, G. Giraud, and J. M. Luck, J. Phys. A **19**, 3153 (1986); A. L. R. Bug, G. S. Grest, and M. H. Cohen, *ibid.* **19**, L323 (1986).
[18] B. E. Springett, Phys. Rev. Lett. **31**, 1463 (1973); I. I. Fishchuk, Phys. Status Solidi A **93**, 675 (1986).
[19] W. H. Press, S. A. Teukolsky, W. T. Vetterling, and B. P. Flannery, *Numerical Recipes*, 2nd ed. (Cambridge University Press, Cambridge, U.K., 1992).
[20] A. R. Mehrabi and M. Sahimi, Phys. Rev. Lett. **79**, 4385 (1997).
[21] *Real-Space Renormalization*, edited by T. W. Burkhardt and J. M. J. van Leeuwen (Springer-Verlag, Berlin, 1982).
[22] J. Bernasconi, Phys. Rev. B **18**, 2185 (1978); C. Tsallis, A. Coniglio, and S. Redner, J. Phys. C **16**, 4339 (1983).
[23] A. Heidarinasab, B. Dabir, and M. Sahimi, Atmos. Environ. **38**, 6381 (2004).
[24] F. Ebrahimi and M. Sahimi Transp. Porous Media **57**, 75 (2004).